https://doi.org/10.1016/j.buildenv.2018.05.010

Title: Investigation on the dehumidification performance of LiCl/H_2O-MWNTs nanofluid in a falling film dehumidifier

Author: Tao Wen, Lin Lu * (vivien.lu@polyu.edu.hk), Hong Zhong

Renewable Energy Research Group, Department of Building Services Engineering, The Hong Kong Polytechnic University, Hong Kong, China

Abstract: Nanofluids could enhance both the heat and mass transfer performance due to its outstanding thermal properties. However, most previous studies only focused on the heat transfer while the mass transfer performance of nanofluids is seldom examined. In the paper, it proposed a novel LiCl/H_2O-MWNTs nanofluid for dehumidification by adding multi-walled carbon nanotubes (MWNTs) into Lithium chloride (LiCl) solution. The stable LiCl/water-MWNTs nanofluid was prepared by adding surfactant polyvinyl pyrrolidone (PVP) through mechanical methods. The concentration of MWNTs and PVP were 0.1 wt% and 0.4 wt% respectively. The influences of various parameters on dehumidification performance of LiCl/H_2O solution, LiCl/H_2O-PVP solution and LiCl/H_2O-MWNTs nanofluid were investigated and compared. The experimental results show that LiCl/H_2O-PVP solution and nanofluid can enhance the dehumidification rate by up to 26.1% and 25.9% as a result of contact angle reduction. The contact angles decrease from 58.5^o for LiCl solution to 28^o and 26.5^o for the two modified solutions respectively, the wetting areas increase from 0.172m^2 to 0.209m^2 and 0.210m^2, and the film thickness reduces from 0.681mm to 0.583mm and 0.577mm correspondingly. However, the dehumidification enhancement of nanofluid can be only attributed to the adding of surfactant, and the adding of 0.1wt% MWNTs has undetected effect on the dehumidification performance in the present study. The results can provide some guidance for the mass transfer enhancement in liquid desiccant dehumidification in terms of adding surfactant and nanoparticle.

Key words: surfactant, MWNTs, nanofluid, dehumidification, falling film

Nomenclature			
d	Absolute humidity(g/kg)	Greek symbols	
G	Mass flow rate(kg/s)	φ	Relative humidity(%)
h	Enthalpy(kJ/kg)	ρ	Density(kg/m^3)
LDCS	Liquid desiccant cooling system	Δ	Change value
LiCl	Lithium Chloride	Subscripts	
MWNTs	Multi-walled carbon nanotubes	a	Air
Δm	Dehumidification rate (g/s)	dry	Dry bulb
PVP	Polyvinyl pyrrolidone	i	Inlet
T	Temperature(^{o}C)	o	Outlet
VCS	Vapor compression system	s	Solution
X	Concentration(%)	w	Cooling water

1 Introduction

Liquid desiccant cooling system (LDCS) has been considered as a promising alternative for the conventional vapor compression cooling system (VCS) [1]. Different with the VCS who removes the humidity load by cooling the temperature of processing air under dew point temperature, the LDCS absorbs the extra water vapor of the processed air through the partial water vapor pressure difference between the air and liquid desiccant. In consequence, it deals with the latent load individually by the sources of solar energy or waste heat, which leads to higher system efficiency and more comfortable indoor environment. Dehumidifier, as a key component in the LDCS, plays the role of water vapor absorption and influences the system performance notably. Therefore, how to improve the dehumidification performance becomes a meaningful focus for researchers.

Generally speaking, the mass enhancement technologies can be classified into two main types: physical method and chemical method. The former one improves the mass transfer by enhancing the wettability of contact surface with structure modification [2-4] or strength the turbulence of liquid film with mechanical disturbance [5, 6]. For the latter one, the wettability of contact surface is improved with chemical techniques, such as surface treatment by super hydrophilic coating [1, 7], and the addition of surfactant [8, 9] or nanofluid [10, 11]. The present study put its concentration on the adding of nanofluid and related investigations in this field will be presented in the following.

Nanofluid is defined to be the stable lyosol with ultrafine particles of diameter less than 100nm [12]. It is fabricated by dispersing nanoparticles into base fluid through mechanical and chemical methods. In recent years, it has drawn more and more attention since it was observed with enhancement in heat and mass transfer [10, 11]. For heat transfer, various degrees of enhancement were found for water and other base fluids with the adding of different kinds of nanoparticles, such as Cu, Al_2O_3, Fe, SiO_2 [13, 14]. Compared with the attention drawn in heat transfer, the study on mass transfer of nanofluids is still limited.

Some investigators studied the bubble absorption characteristics of nanofluids [15-21]. Kim et al. [15] investigated the effects of three different kinds of nanoparticles on the absorption performance in NH_3/H_2O solution. Their experimental results indicated that the absorption performance could be increased up to 3.21 times. Among the three kinds of particles, i.e., Cu, CuO and Al_2O_3, Cu was the most effective candidate. They contributed the absorption enhancement to the grazing effect proposed by Alper et al. [16]. Furthermore, Kim et al. [17] studied the effect of adding both surfactants and nano-particles to NH_3/H_2O on the behavior of bubble absorption. 2-ehtyl-1-hexanol, n-octanol and 2-octanol were employed as the surfactants. 5.32 times absorption rate improvement was observed with both 2-ehtyl-1-hexanol and Cu nano-particles. They recommended that the mass transfer performance could be improved significantly by adding surfactant and nano-particles simultaneously. Similar experiments were carried out by Ma et al. [18], who adopted carbon nanotubes (CNTs) as the nanoparticles. They stated that by using the surface treatment chemical method, the CNTs were dispersed into NH_3/H_2O solution evenly. Different from the conclusion drawn by Kim et al. [17] that the absorption improvement increased with the increase of nanoparticles concentration, Ma et al. [18] considered that there was an optimum particle concentration to achieve the highest absorption rate. In addition to the abovementioned nanoparticles, SiO_2 [19], Fe_3O_4 [20] and Ag [21] were also added into base fluids such like methanol for the purpose of mass transfer enhancement. Different levels of absorption enhancement were found in these studies.

Besides the bubble type absorption, falling film absorption is another type of mass transfer which is usually used in CO_2 absorption and absorption refrigeration systems [10]. Kang et al. [22] experimentally measured the water vapor absorption rate with the adding of Fe and CNTs nanoparticles of 0, 0.01% and 0.1wt% in a tube falling film absorber. Their results revealed that the absorption rate was larger at higher concentration of nanoparticle. What is more, the addition of CNTs presented better mass transfer performance than Fe nanoparticle. The average mass transfer enhancement for 0.1 wt% CNTs could reach up to 2.48 times. In their study, surfactant named Arabic gum were used to get stable nanofluid by the means of ultrasonic vibrator. However, they did not investigate the effect of Arabic gum on mass transfer characteristics alone. Three kinds of nanoparticles, namely Al_2O_3, Fe_2O_3 and $ZnFe_2O_4$, were added into ammonia/water solution to study the ammonia absorption performance by Yang et al. [23]. They added sodium dodecyl benzene sulfonate (SDBS) into ammonia/water solution as surfactant. After that, mechanical agitation and ultrasonic vibration were exerted on the solution to obtain even and steady nanofluid. Different from the work done by Kang et al. [22], they investigated the influence of SDBS on absorption rate at first and pointed out that the absorption rate decreased with the increase of SDBS concentration. Then, the influence of nanoparticles on absorption was studied. Results showed that the absorption rate could only increase when the nanoparticles were evenly and stably dispersed in base fluid. The increment of effective absorption rate by adding Fe_2O_3 and $ZnFe_2O_4$ could be 0.7 and 0.5 respectively under certain operating conditions. Pineda et al. [24] investigated the CO_2 absorption characteristics by methanol with the adding of Al_2O_3 and SiO_2 nanoparticles. They used the sonication to disperse nanoparticles into methanol. Their experimental data indicated that the absorption rates were enhanced by up to 9.4% and 9.7% at the concentration of 0.05 %vol for Al_2O_3 and SiO_2 individually. In the work done by Kim et al. [25], they stated that the distribution stabilizer was required for the stable dispersion of nanofluid when the concentration of SiO_2 nanoparticle was greater than 0.01 %vol. They also carried out experiments to study the vapor absorption rate of LiBr/H_2O soluiton with 0.005 %vol SiO_2

nanoparticles and 18% absorption enhancement was detected from their experiment results. In addition to experimental study, numerical investigation was also adopted by previous researchers [26, 27]. Ali et al. [26, 27] numerically studied the heat and mass transfer performance of liquid desiccant by adding Cu-ultrafine particles.

From the foregoing literature review, it is found that even though there are some studies related to the mass transfer with nanofluid applied in bubble absorption [15-21] and absorption refrigeration [22-23, 25], no works on liquid desiccant dehumidification were reported. What is more, according to the research by Yang [23] and Kim [25], the adding of surfactants for nanofluid stability plays an important role in the mass transfer process. However, some researchers failed to investigate the effect of surfactant on the mass transfer alone, such as Lee et al. [19] and Kang et al. [22]. The present study focused on the dehumidification performance of $LiCl/H_2O$ solution with the addition of multi-walled carbon nanotubes (MWNTs). The even and steady $LiCl/H_2O$-MWNTs nanofluid was firstly prepared by adding PVP surfactant with mechanical methods. Then the dehumidification performances of adding PVP to solution and adding nanofluid to solution were identified separately. In order to uncover the mass transfer enhancement mechanism, parameters, such as wettability, contact angle of solution, film thickness and thermal conductivity, were measured and compared.

2 $LiCl/H_2O$-MWNTs nanofluid preparation

The MWNTs used in present study were purchased from Suzhou Hengqiu Graphene Co. LTD. They have the inner diameter of 3-5 nm and outer diameter of 8-15 nm. Their lengths range from 3 to 12 um. The SEM image of MWNTs is shown in Fig. 1. The MWNTs usually intertwine with each other. Therefore, under normal conditions, it is hard to disperse nanoparticles in base fluid evenly and stably, which was also addressed by Kim et al. [25]. In practice, various methods, such as mechanical agitation, grinding, ultrasonic vibration and chemical stabilizer, are adopted to obtain stable nanofluid [28]. After various attempts, the present study chose polyvinyl pyrrolidone (PVP) as the surfactant to get stable nanofluid. In order to select appropriate concentration of PVP, concentration from 0.1 to 0.4 wt% were

tested. The PVP was firstly dissolved in LiCl solution by mechanical agitation. Subsequently, the MWNTs were added into the solution with 1 hour stirring at 1300 rpm. After that, 2 hours' ultrasonic vibration was exerted on the previous solution. The prepared solutions with the adding of 0.1 wt% MWNTs at the PVP concentrations of 0, 0.1, 0.2, 0.3, 0.4 wt% were shown in Fig. 2-a. After 60 days' static settlement, it was found that MWNTs deposited completely if no PVP was added. When the concentration of PVP was less than 0.4 wt%, different degrees of sediment were observed as shown in Fig. 2-b. As a contrast, the solution with 0.4 wt% PVP showed good stability without obvious deposits. In order to illustrate the dispersion characteristics of solution, TEM test for solution was carried out and the image was shown in Fig. 3. From it, one can see that the MWNTs were no longer clustered. They were finely and highly dispersed into LiCl/H_2O solution by adding PVP with mechanical dispersion methods.

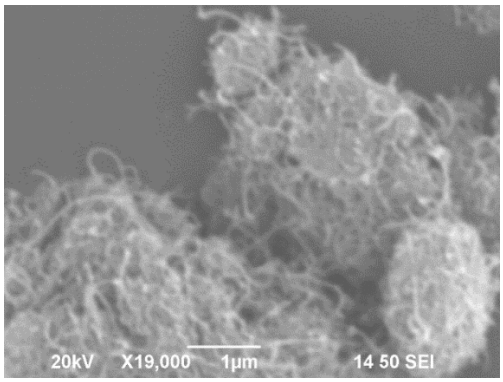

Fig. 1. SEM image of the MWNTs.

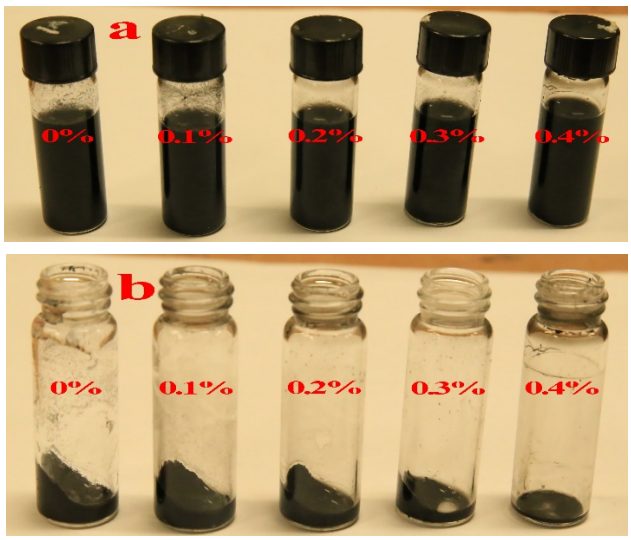

Fig. 2. Dispersion results under different PVP concentration: (a) 0 day, (b) 60 days.

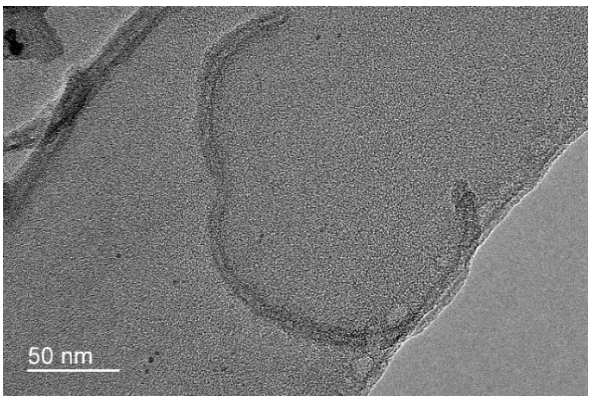

Fig. 3. TEM image of the LiCl/H_2O-MWNTs nanofluid.

After the validation of nanofluid fabrication methods, LiCl/H_2O-MWNTs nanofluid with the weight of 30kg was prepared for the dehumidification experiments. The strong concentration of nanofluid was produced at first and then diluted to the desired concentration of 0.1 wt%. The fabrication processes and technologies were shown in Fig. 4.

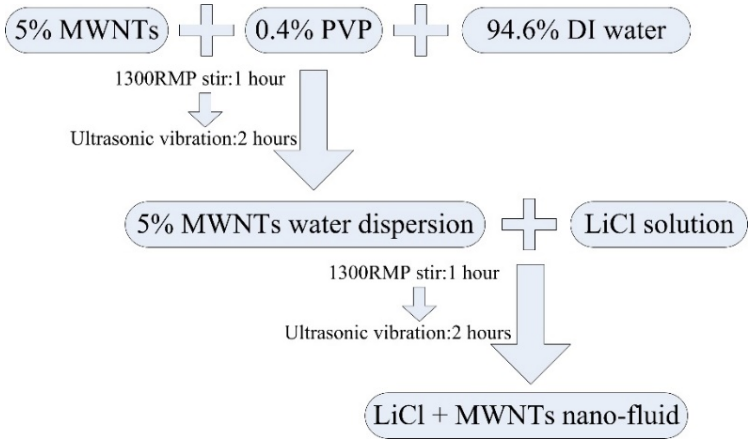

Fig. 4. Fabrication processes for LiCl/H_2O-MWNTs nanofluid.

3 Dehumidification experimental method

3.1 Experimental apparatus

An experimental system with three different loops, namely solution loop, processing air loop and cooling water loop, was designed and built to investigate the influences of different operating parameters on dehumidification performance [29]. The particular system configuration was shown in Fig. 5. These three different loops were distinguished by the color of arrows. All air ducts and fluid pipes were wrapped by neoprene foam with the purpose of thermal isolation. A plane plate made of stainless steel 316L was chosen as the single channel dehumidifier with the size of

500mm*500mm (Length*Width). Fig. 6 illustrates the specific configuration of the single channel dehumidifier. A transparent cover was used to separate the liquid desiccant falling film with the ambient air and made sure the processed air flowed in the channel.

Desiccant solution was stored at a tank which was connected with a pump through plastic pipe. An electrical heater controlled by a Proportion-Integration -Differentiation (PID) controller was installed in the tank to regulate the inlet solution temperature. The solution was pumped from the tank and flowed through a three-way valve firstly. By adjusting the opening of the valve, the solution flow rate could be controlled. The exact value of flow rate was measured by a turbine flow rate sensor installed in the pipe. When the distributor was fully filled with solution, the solution would spill from the horizontal slot in the distributor and flowed along the single channel dehumidifier. After that, the solution was collected by a collector and flowed back to another tank. These two solution tanks were connected with each other by plastics pipe with a pump in the middle. The solution can be pumped to another tank by the pump if necessary. For the processed air loop, the air was driven by an axial flow fan to the air duct. Before flowing into the dehumidifier, its temperature and humidity were adjusted to the required values by an electrical heater and a humidifier individually. The flow rate of air was regulated by a damper installed in the duct. In the dehumidifier, moist air contacted with heavy liquid desiccant in the form of counter current flow. Heat and mass transfer processes would occur driven by the temperature and partial water vapor differences between air and solution. After that, the air flowed out of duct. In order to alleviate the dehumidification efficiency reduction, internal cooling was adopted in present study. Water was cooled by a water chiller and pumped to the loop by a centrifugal pump. After the heat exchange with solution, the water flowed back to the chiller for the next circulation.

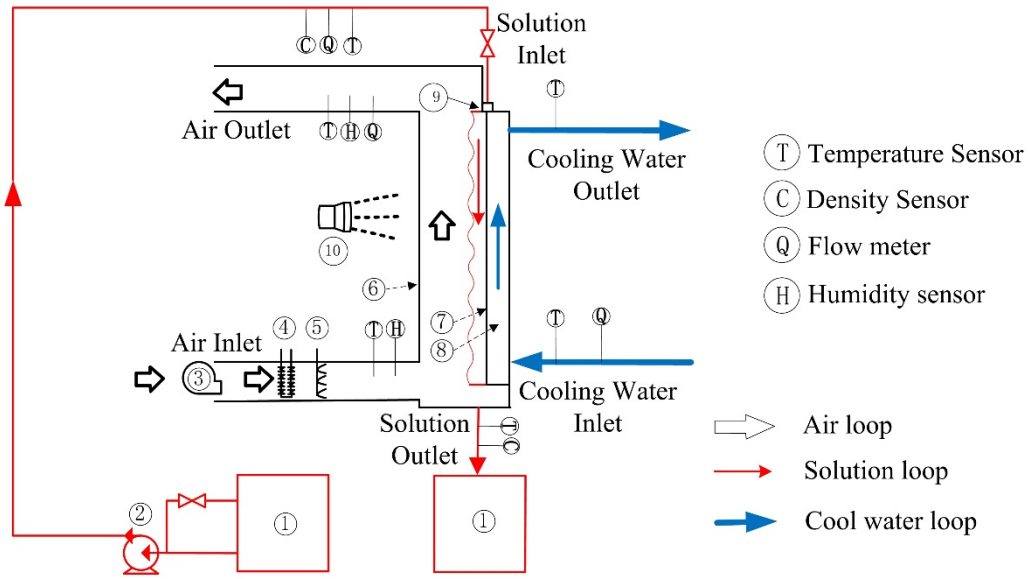

1、Solution tanks 2、Solution pump 3、Air fan 4、Air heater 5、Humidifier 6、Air channel 7、Working surface 8、Internally cooling unit 9、Solution distributor 10、Infrared thermal imager

Fig. 5. Schematic diagram of the test rig.

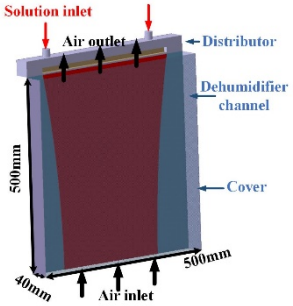

Fig. 6. Specifications of the single channel dehumidifier.

3.2 Experimental data measurement and processing

During the experiments, all the temperatures, including solution inlet and outlet temperatures, cooling water inlet and outlet temperatures, were obtained by Pt-100 thermocouples with the accuracy of 0.1K. Both the solution and cooling water flow rates were measured by turbine flow rate sensors with the accuracy of 3%. For the air flow rate, it was measured by a pitot tube which was connected with a micro-manometer for the sake of air velocity measurement. The air mass flow rate was calculated by the air velocity multiplied with the flow area and density. The concentration of solution was obtained by an indirect way. The solution density was firstly measured by a specific gravity hydrometer with the accuracy of 1kg/m^3. Combined with the solution temperature obtained by Pt-100 thermocouple, the

concentration was uniquely determined by the equation provided by Conde [30]. Two humidity sensors made by E+E Elektronik company and installed at the inlet and outlet of air duct were used to measure the relative humidity and dry bulb temperatures of air. The measurement accuracy was 0.1K for temperatures and 2.5% for relative humidity. The absolute moisture content was calculated by the conversion equation shown in Equation (1).

$$d = f(T_{dry}, \varphi) \tag{1}$$

in which, T_{dry} denotes the dry bulb temperature of air. φ stands for the relative humidity of air.

The dehumidification rate which has been widely adopted by previous researchers was selected in present study to evaluate the dehumidification performance under various circumstances. It indicated the total amount of water vapor absorbed by desiccant solution from moist air. The definition is shown in Equation (2).

$$\Delta m = G_a.(d_{a,o} - d_{a,i}) \tag{2}$$

where G_a means the air mass flow rate. $d_{a,o}$ and $d_{a,i}$ represent the absolute moisture content of inlet and outlet air respectively.

During the data processing, all experimental data can be divided into two groups, namely directed measured ones and calculated ones. The uncertainties of the directed measured ones were determined by the accuracy of sensors. When determining the uncertainties of the calculated ones, such as solution concentration and dehumidification rate, the uncertainty propagation method [31] was adopted as shown in Equation (3).

$$\delta Y = \sqrt{(\frac{\partial Y}{\partial x_1}\delta x_1)^2 + (\frac{\partial Y}{\partial x_2}\delta x_2)^2 + ... + (\frac{\partial Y}{\partial x_n}\delta x_n)^2} \tag{3}$$

in which, δY is the uncertainly of the calculated parameter Y. δx_n means the uncertainty of the n_{th} measured parameter. According to the accuracy of sensors and Equation 3, all the uncertainties of parameters were obtained and presented in Table 1.

Table 1. The uncertainties of different parameters.

Parameter	Uncertainty	Parameter	Uncertainty
Temperature/ T	± 0.1K	Cooling water flow rate/ G_w	± 3%
Solution flow rate/ G_s	± 3%	Solution concentration/ X_s	0.2%
Solution density/ ρ_s	± 1kg/m^3	Air absolute humidity/ d	2.5%
Air flow rate/ G_a	± 2.2%	Dehumidification rate/ Δm	5.0%
Air relative humidity/ φ	± 2.5%		

3.3 Experimental system validation and operating conditions

In the single channel dehumidifier, the moist processed air flows in contact with the liquid desiccant along with the simultaneous heat and mass transfer. During such processes, energy and mass conservation must be satisfied which are formulated by Equations (4) and (5).

$$G_s(h_{s,o}-h_{s,i})+G_a(h_{a,o}-h_{a,i})=G_w(h_{w,i}-h_{w,o}) \quad (4)$$

$$G_a(d_{a,i}-d_{a,o})=G_sX_{s,i}(\frac{1}{X_{s,o}}-\frac{1}{X_{s,i}}) \quad (5)$$

where G, h and X stand for the mass flow rate, enthalpy and solution concentration severally. s, a and w in the subscript correspond to the solution, air and cooling water. Letters i, o in the subscript distinguish the inlet and outlet parameters.

The energy balance equation shown in Equation (4) could be checked by measuring the mass flow rate and temperature of fluids. However, Equation (5) for mass balance was unlikely to be validated because of the undetected change of solution concentration in one cycle. In consequence, only the energy conservation expressed by Equation (4) was validated in present study and the results are shown in Fig. 7. From the figure, we can see most of the energy differences between the right side and left side of Equation (4) are less than ±25%. According the previous references, the absolute energy differences always falling into the error band of 0~30% [32-34]. The energy differences are caused by the uncertainties of the measured parameters and also the small amount of heat exchange between the experimental system and ambient environmental. In terms of the foregoing description, the experimental system is proven reasonably for the subsequent investigation.

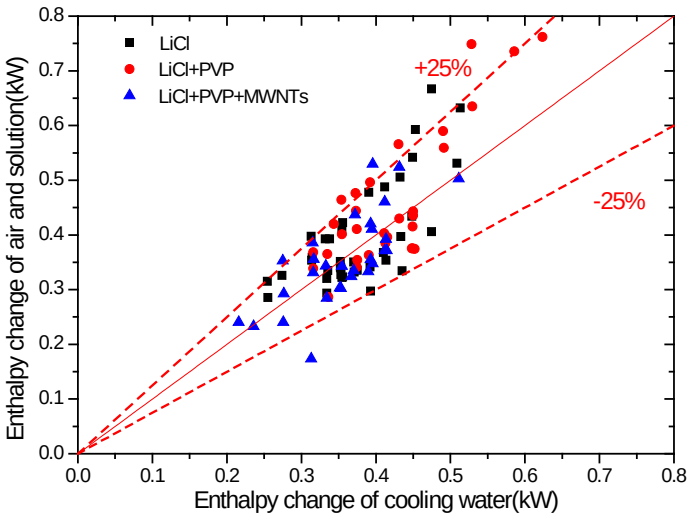

Fig. 7. Energy balance of the experimental system.

During the experiments, the concentration of liquid desiccant was kept at 35%, and the concentrations of MWNTs and PVP were maintained at 0.1 % wt and 0.4 wt% respectively. For the cooling water, its mass flow rate and inlet temperature were kept at 0.12kg/s and 18°C. Other parameters, such as air flow rate, inlet humidity, inlet dry bulb temperature and solution mass flow rate and inlet temperature, were changed in the ranges shown in Table. 2.

Table. 2. Summary of the experimental operating conditions.

Material	Parameter	Range
Solution	Concentration (wt%)	35
	Mass flow rate (kg/s)	0.082~0.16
	Inlet temperature (°C)	28~35
Processing air	Inlet humidity (g/kg)	16~24.7
	Mass flow rate (kg/s)	0.023~0.067
	Inlet temperature (°C)	29~37
Cooling water	Mass flow rate (kg/s)	0.12
	Inlet temperature (°C)	18
PVP	Concentration (wt%)	0.4
MWNTs	Concentration (wt%)	0.1

4 Results and discussion

4.1 Influence of air flow rate on dehumidification rate

The dehumidification rates under the air mass flow rate from 0.023kg/s to 0.067kg/s are shown in Fig. 8. Three different kinds of liquid desiccant, namely normal LiCl/H_2O solution, LiCl/H_2O-PVP solution and LiCl/H_2O-MWNTs nanofluid with PVP surfactant, were investigated individually. For all of the three solutions, the

dehumidification rates show an increase trend with the increase of air flow rate when the air flow rate is less than 0.06kg/s. However, at higher flow rate, for example 0.067kg/s, the dehumidification rate shows a declining trend. An explanation for such trends is that the dehumidification rate formulated by Equation 2 is the product of the air flow rate and absolute moisture removal (the absolute moist content different between the inlet and outlet processed air). As one can see, the absolute moist content always decreases with the increase of air flow rate. When the air flow rate is less than 0.06kg/s, the increment of air flow rate overwhelms the decrement of absolute moist removal. Therefore, the dehumidification rate shows an ascending trend. However, beyond the flow rate of 0.06kg/s, the decrement of absolute moisture removal overwhelms the increment of air flow rate and shows greater influence on dehumidification rate as demonstrated in Fig. 9. Therefore, under the co-effect of both the air flow rate and absolute moist removal, the dehumidification rate has an ascending tendency at air flow rate lower than 0.06kg/s and a descending trend at higher air flow rate. Compared with the LiCl/H_2O solution, the other two kinds of solution have an obvious improvement in terms of dehumidification rate. For example, when the air mass flow rate is 0.042kg/s, the dehumidification rate for LiCl/H_2O solution is 0.0906g/s. While the values are 0.106g/s and 0.108g/s for LiCl/H_2O-PVP solution and LiCl/H_2O-MWNTs nanofluid severally. The relative improvements are 17.0% and 19.2% correspondingly. Overall, the adding of 0.1 wt% MWNTs does not contribute to a detected improvement in mass transfer. The dehumidification rates are more or less the same for LiCl/H_2O-PVP solution and LiCl/H_2O-MWNTs nanofluid under the same working conditions.

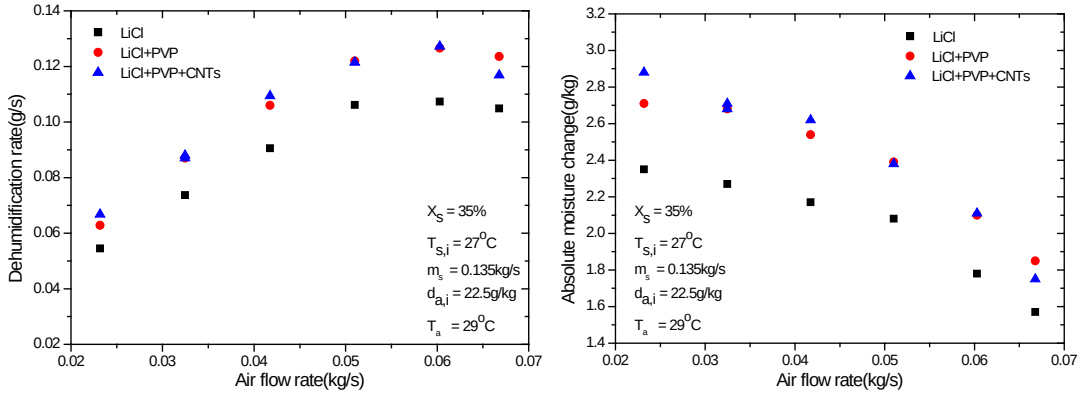

Fig. 8. Influence of air flow rate on dehumidification performance. (Left)

Fig. 9. The absolute moist removal under different air flow rates. (Right)

4.2 Influence of air inlet humidity on dehumidification rate

Fig. 10 illustrates the effect of air inlet humidity on dehumidification rate. When the air inlet humidity increases from 17g/kg to 24.7g/kg, the dehumidification rate also increases from 0.036 g/s to 0.091kg/s under the working conditions for $LiCl/H_2O$ solution. Similar tendencies can also be observed for the other two kinds of solutions. The phenomenon can be explained by the growth of mass transfer driving force with the increase of air humidity when the solution concentration keeps constant. During the mass transfer process, the driving force is the partial water vapor pressure difference between the processed air and solution. Higher humidity corresponds to bigger partial water vapor pressure and leads to greater mass transfer force. By adding PVP, the dehumidification rate shows a distinct increase which is indicted in Fig. 10. However, the adding of MWNTs into $LiCl/H_2O$-PVP solution has negligible influence on dehumidification performance in present study as shown in Fig. 10.

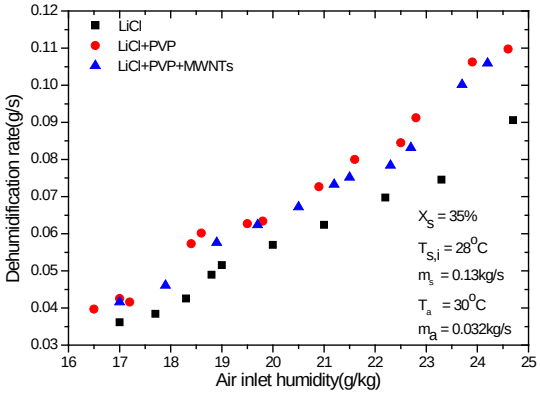

Fig. 10. Influence of air humidity on dehumidification performance.

4.3 Influence of air inlet temperature on dehumidification rate

The influence of air inlet dry bulb temperature on dehumidification characteristics is illustrated in Fig. 11. The dehumidification rates fluctuate around the values of 0.0671g/s, 0.0861g/s and 0.0849g/s for the abovementioned three kinds of solution when the temperature of air changes from 29°C to 37°C. No distinct trends for dehumidification rate can be concluded from Fig. 11 under different air temperatures. The reason is that under change of air temperature in present study, the mass transfer coefficient between air and solution almost keeps the same around 0.25kg/(m^2.s), 0.309 kg/(m^2.s) and 0.30 kg/(m^2.s) for the three kinds of solution. Relative enhancements of 28.3% and 26.5% are obtained for $LiCl/H_2O$-PVP solution

and LiCl/H_2O-MWNTs nanofluid respectively. Compared with the experimental data of LiCl/H_2O-PVP solution, the dehumidification rate for LiCl/H_2O-MWNTs nanofluid does not show much difference and even has a slight decrease.

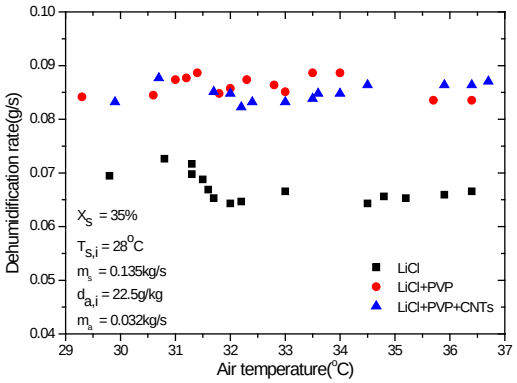

Fig. 11. Influence of air temperature on dehumidification performance.

4.4 Influence of solution flow rate on dehumidification rate

As shown in Fig. 12, the effect of solution flow rate on dehumidification rate is presented. Even though the mass flow rate of solution has a nearly 100% increase from 0.082kg/s to 0.16kg/s, the dehumidification rates maintain around 0.0692g/s, 0.0865g/s and 0.0867g/s for the three solutions. Therefore, we can conclude that the solution flow rate does not influence the dehumidification performance under the operating conditions of present study. Compared with the dehumidification rate of LiCl/H_2O solution, the average relative enhancement for dehumidification rate is 25.0% and 25.3% for the other two solutions. It is obvious that the enhancement degrees for the two modified solutions are almost the same, which indicates that the adding of MWNTs into LiCl/H_2O-PVP solution almost does not affect the mass transfer performance.

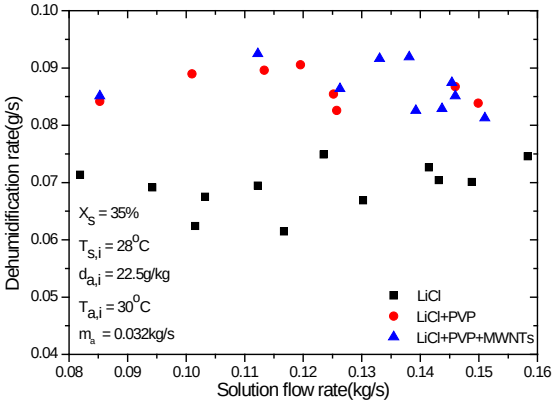

Fig. 12. Influence of solution flow rate on dehumidification performance.

4.5 Influence of solution inlet temperature on dehumidification rate

From Fig. 13, the dehumidification rate at different solution temperatures can be obtained. It is obvious that the dehumidification rates decrease with the increment of solution temperature. When the LiCl/H_2O solution inlet temperature increases from 28°C to 35 °C, the dehumidification rate has a reduction of 0.0154g/s from 0.0698g/s to 0.0544g/s. For LiCl/H_2O-PVP solution and LiCl/H_2O-MWNTs nanofluid, the decrements are 0.0205g/s from 0.0864g/s to 0.0659g/s and 0.026g/s from 0.088g/s to 0.064g/s respectively. The reduction in terms of dehumidification rate can be contributed to the increment of the partial water vapor pressure at the surface of solution when solution temperature has an increment. The dehumidification rate has an obvious improvement under the same operating conditions for both the two modified solutions as demonstrated by Fig. 13. In line with the previous phenomenon, the adding of MWNTs does not show up a distinct effect on the dehumidification characteristics.

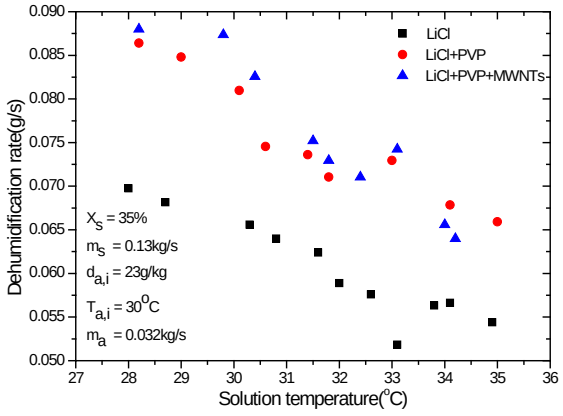

Fig. 13. Influence of solution temperature on dehumidification performance.

4.6 Discussion

From the experimental data from Fig. 8 to Fig. 13, the conclusion is that the LiCl/H_2O-PVP solution and LiCl/H_2O-MWNTs nanofluid can significantly improve the dehumidification performance. Averagely speaking, the relative enhancements are 26.1% for the LiCl/H_2O-PVP solution and 25.9% for nanofluid under the same working conditions. In order to investigate the mechanism of the dehumidification enhancement, the wettability was measured as well due to its obvious difference present for different solutions. A high resolution infrared thermal imager from FLUKE company was empolyed to measure the wetting area of solution on the plate

dehumidifiers. The results are shown in Fig. 14. Compard with the distinct film shrinkage for LiCl/H_2O solution on dehumidifier, the other two solutions can wet the surface greatly without obvious film contraction. The wetting area increases from 0.172m^2 for LiCl/H_2O solution to 0.209m^2 and 0.210m^2 with a relative increment of 21.5% and 22.0% for LiCl/H_2O-PVP solution and LiCl/H_2O-MWNTs nanofluid severally. Apparently, the increment of wetting area leads to bigger mass transfer contact area between solution and processed air and greater dehumidification rate subsequently. For the improvement of wettability, it can be contributed to the decrease of contact angles of solutions on dehumidifier which were measured by a standard contact angle goniometer made by Rame-hart instrument Co. with the accuracy of 0.1^o. The contact angles of the three kinds of solutions were presented in Fig. 15. A remarkable reduction of 30.5^o from 58.5^o to 28^o was observed when adding 0.4 wt% PVP into LiCl/H_2O solution. The contact angle for nanofluid is nearly the same as LiCl/H_2O-PVP solution with a difference of 1.5^o which consists with the wetting area increment mentioned above. It is worth noting that the relative percentage of wettability improvement of 21.5% and 22.0% is slightly smaller than that of the dehumidification rate enhancement of 26.1% and 25.9% for LiCl/H_2O-PVP solution and LiCl/H_2O-MWNTs nanofluid respectively. The further improvement proportion is attributed to the decrement of falling film thickness. The falling film thickness was also measured by the help of a JDC-2008 accumeasure instrument developed by TianJin Univesity with the accuracy of 0.8 μm. The outcomes are given in Table 3. Compared with the LiCl/H_2O solution film thickness of 0.681mm, the other two solutions have a film thickness reduction of 0.1mm approximately. Thinner film thickness results in smaller heat transfer resistance between solution and cooling water and higher efficiency of internal cooling. Consequently, the dehumidification rate will be enhanced at thinner film thickness.

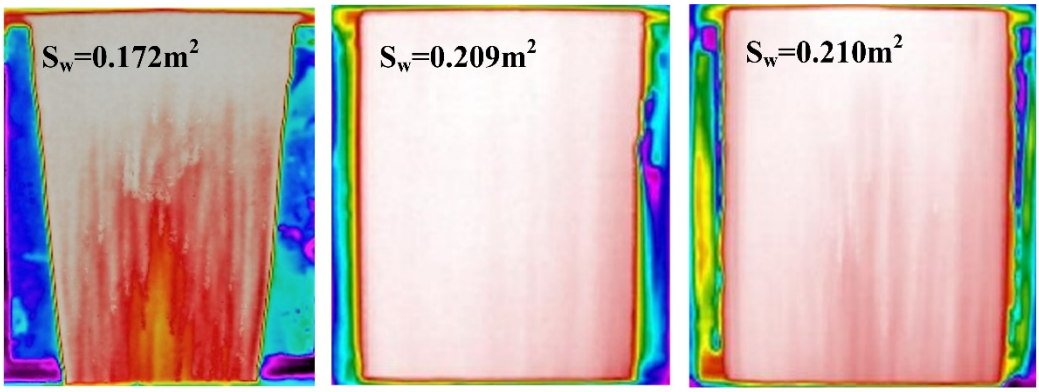

Fig. 14. Wettability of different solutions on dehumidifiers.

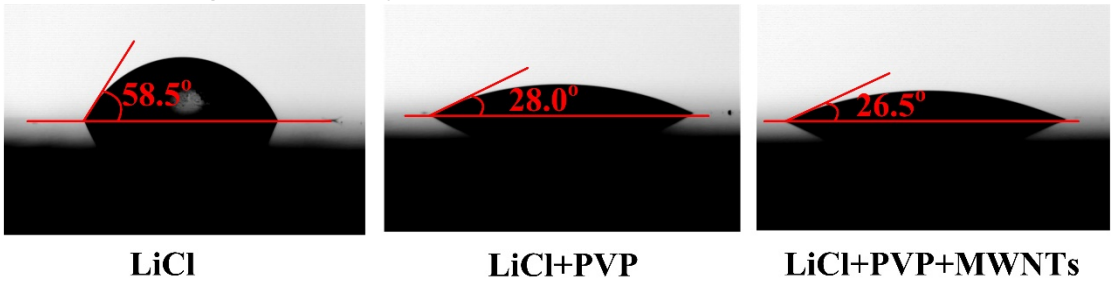

Fig. 15. Contact angles of diffenent solutions on plate dehumidifier

Table. 3. Average film thickness of falling film for different solutions

Solution	Average film thickness(mm)
LiCl	0.681
LiCl + PVP	0.583
LiCl + PVP + CNTs	0.577

To sum up, the average relative dehumidification rate enhancements for the LiCl/H_2O-PVP solution and nanofluid are 26.1% and 25.9%. For both solutions, the enhancement is mainly resulted for the increment of wetting area and partially from the decrement of falling film thickness as stated above. The enhancement degrees are very close to each other for these two solutions and it means that the adding of 0.1 wt% MWNTs into LiCl/H_2O-PVP solution has negligible influence on the mass transfer performance in present study. To explore the reason, the thermal conductivity, regarded as an important factor for the heat and mass transfer enhancement in previous researchers [13, 14], was also obtained by Thermal Conductivity Meter-TC3000E. It has the resolution of 0.001W/(m.K) and accuracy of 2%. The detailed results which include both the validation data and measurements are specified in Table. 4. From the table, the accuracy of the thermal conductivity meter can be validated by the experimental data of water measured twice. The relative deviation between measured valued values and reference values [35] are 1.28% and 0.02%

respectively. After the validation, the thermal conductivity of LiCl/H_2O solution and LiCl/H_2O-MWNTs nanofluid were measured individually. As one can see from Table. 4, the relative differences between these two solutions are both 0.5% which shows that the adding of 0.1% MWNTs has almost no effect on the thermal conductivity. The undetected thermal conductivity improvement is in line with the negligible effect of MWNTs on mass transfer performance. So it is concluded that PVP is an indispensable surfactant for the steady dispersion of MWNTs into LiCl solution. The wettability improvement and film thickness decrement for LiCl/H_2O-MWNTs nanofluid compared with normal LiCl solution is caused by the addition of surfactant PVP. The adding of MWNTs has negligible influence on these properties and dehumidification performance as well.

Even though the LiCl/H_2O-MWNTs nanofluid can increase the dehumidification rate up to 25.9%, the present study contributes such enhancement to the adding of surfactant which is indispensable for the stability of nanofluid rather than the nanoparticle itself. The conclusion is very different from research results mentioned in the foregoing literature review. In the mind of the authors, there are two main reasons which may lead to the discrepancy. One is that several researchers added surfactant into base fluids during the dispersion of nanofluid. However, they failed to investigate the effect of surfactant on the mass transfer characteristic alone. The other one is that the research of present study is liquid desiccant dehumidification. All the experiments were conducted under atmospheric pressure while most the research on falling film absorption was concerned about absorption refrigeration which was conducted under pressures far less than atmospheric pressure, i.e., 1kPa [22, 25]. Consequently, the significant difference in terms of operating pressure may be another reason.

Table. 4. Thermal conductivity measurement results

	Test time	Water	Reference value[35]	Relative deviation
Validation	First time	0.6150	0.6072	1.28%
(Unit: W/(m.k))	Second time	0.6073	0.6072	0.02%
	Test time	LiCl	LiCl+MWNTs	Relative difference
Measurement	First time	0.5405	0.5428	0.43%
(Unit: W/(m.k))	Second time	0.5420	0.5439	0.19%

5 Conclusion

The stable LiCl/H_2O-MWNTs nanofluid was fabricated by the help of PVP

surfactant and mechanical methods. The dehumidification rates of three kinds of solutions, namely LiCl/H_2O solution, LiCl/H_2O-PVP solution and LiCl/H_2O-MWNTs nanofluid, were identified and compared under various operating conditions. The main conclusions are drawn as follows:

(1) The adding of 0.4 wt% surfactant PVP into LiCl/H_2O solution reduces the contact angle from 58.5^o to 28^o. Correspondingly, the falling film thickness has a reduction of 0.1mm nearly. The wetting area increases from 0.172m^2 to 0.209m^2 with a relative increment of 21.5%. When adding 0.1 wt% MWNTs into the LiCl/H_2O-PVP solution, almost the same results are observed in terms of contact angle, film thickness and wetting area. The thermal conductivity of LiCl/H_2O-MWNTs nanofluid with the 0.1 wt% MWNTs has negligible change compared with LiCl/H_2O solution.

(2) The dehumidification rate is the co-effect result of both air flow rate and absolute moist removal. It increases with the increase of air flow rate when the air flow rate is less than 0.06kg/s due to the overwhelming effect of air flow rate. However, at higher air flow rate, it has the descending potential caused by the remarkably decrement of absolute moist removal.

(3) The average relative increment of dehumidification rates are 26.1% and 25.9% respectively for LiCl/H_2O-PVP solution and LiCl/H_2O-MWNTs nanofluid due to the significant decrease of contact angle and improvement of wettability.

(4) The adding of 0.4 wt% PVP surfactant along with high speed agitation and ultrasonic vibration helps to get stable LiCl/H_2O-MWNTs nanofluid. However, the dehumidification enhancement of nanofluid can only be attributed to the adding of surfactant. The adding of 0.1 wt% MWNTs shows negligible influence on dehumidification performance.

Acknowledgement

The work is financially supported by Hong Kong Research Grant Council through General Research Funds (PolyU 152010/15E and PolyU 152184/17E).

References

[1] Dong C., Lu L., Qi R., Model development of heat/mass transfer for internally cooled dehumidifier concerning liquid film shrinkage shape and contact angles, Building and Environment, 114 (2017) 11-22.

[2] Mortazavi M., Isfahani R.N., Bigham S., Moghaddam S., Absorption characteristics of falling film LiBr (lithium bromide) solution over a finned structure, Energy, 87 (2015) 270-278.

[3] Luo Y., Shao S., Xu H., Tian C., Yang H., Experimental and theoretical research of a fin-tube type internally-cooled liquid desiccant dehumidifier, Applied Energy, 133 (2014) 127-134.

[4] Yin Y., Zhang X., Wang G., Luo L., Experimental study on a new internally cooled/heated dehumidifier/regenerator of liquid desiccant systems, International Journal of Refrigeration, 31 (2008) 857-866.

[5] Park C., Nosoko T., Gima S., Ro S., Wave-augmented mass transfer in a liquid film falling inside a vertical tube, International journal of heat and mass transfer, 47 (2004) 2587-2598.

[6] Yoshimura P., Nosoko T., Nagata T., Enhancement of mass transfer into a falling laminar liquid film by two-dimensional surface waves—some experimental observations and modeling, Chemical Engineering Science, 51 (1996) 1231-1240.

[7] Qi R., Lu L., Energy consumption and optimization of internally cooled/heated liquid desiccant air-conditioning system: A case study in Hong Kong, Energy, 73 (2014) 801-808.

[8] Lin S.J.F., Shigang Z., Experimental study on vertical vapor absorption into LiBr solution with and without additive, Applied Thermal Engineering, 31 (2011) 2850-2854.

[9] Kang B., Kim K., Lee D., Fluid flow and heat transfer on a falling liquid film with surfactant from a heated vertical surface, Journal of mechanical science and technology, 21 (2007) 1807-1812.

[10] Pang C., Lee J.W., Kang Y.T., Review on combined heat and mass transfer characteristics in nanofluids, International Journal of Thermal Sciences, 87 (2015) 49-67.

[11] Ashrafmansouri S.-S., Esfahany M.N., Mass transfer in nanofluids: A review, International Journal of Thermal Sciences, 82 (2014) 84-99.

[12] Chol S., Enhancing thermal conductivity of fluids with nanoparticles, ASME-Publications-Fed, 231 (1995) 99-106.

[13] Yu W., France D.M., Routbort J.L., Choi S.U., Review and comparison of nanofluid thermal conductivity and heat transfer enhancements, Heat Transfer Engineering, 29 (2008) 432-460.

[14] Godson L., Raja B., Lal D.M., Wongwises S., Enhancement of heat transfer using nanofluids—an overview, Renewable and sustainable energy reviews, 14 (2010) 629-641.

[15] Kim J.-K., Jung J.Y., Kang Y.T., The effect of nano-particles on the bubble absorption performance in a binary nanofluid, International journal of refrigeration, 29 (2006) 22-29.

[16] Alper E., Wichtendahl B., Deckwer W.-D., Gas absorption mechanism in catalytic slurry reactors, Chemical Engineering Science, 35 (1980) 217-222.

[17] Kim J.-K., Jung J.Y., Kang Y.T., Absorption performance enhancement by nano-particles and chemical surfactants in binary nanofluids, International Journal of Refrigeration, 30 (2007) 50-57.

[18] Ma X., Su F., Chen J., Bai T., Han Z., Enhancement of bubble absorption process using a CNTs-ammonia binary nanofluid, International Communications in Heat and Mass Transfer, 36 (2009) 657-660.

[19] Lee J.W., Jung J.-Y., Lee S.-G., Kang Y.T., CO 2 bubble absorption enhancement in methanol-based nanofluids, International journal of refrigeration, 34 (2011) 1727-1733.

[20] Wu W.-D., Liu G., Chen S.-X., Zhang H., Nanoferrofluid addition enhances ammonia/water bubble

absorption in an external magnetic field, Energy and Buildings, 57 (2013) 268-277.
[21] Pang C., Wu W., Sheng W., Zhang H., Kang Y.T., Mass transfer enhancement by binary nanofluids (NH 3/H 2 O+ Ag nanoparticles) for bubble absorption process, International journal of refrigeration, 35 (2012) 2240-2247.
[22] Kang Y.T., Kim H.J., Lee K.I., Heat and mass transfer enhancement of binary nanofluids for H 2 O/LiBr falling film absorption process, International Journal of Refrigeration, 31 (2008) 850-856.
[23] Yang L., Du K., Niu X.F., Cheng B., Jiang Y.F., Experimental study on enhancement of ammonia–water falling film absorption by adding nano-particles, International journal of refrigeration, 34 (2011) 640-647.
[24] Pineda I.T., Lee J.W., Jung I., Kang Y.T., CO 2 absorption enhancement by methanol-based Al 2 O 3 and SiO 2 nanofluids in a tray column absorber, International journal of refrigeration, 35 (2012) 1402-1409.
[25] Kim H., Jeong J., Kang Y.T., Heat and mass transfer enhancement for falling film absorption process by SiO 2 binary nanofluids, International Journal of Refrigeration, 35 (2012) 645-651.
[26] Ali A., Vafai K., Khaled A.-R., Analysis of heat and mass transfer between air and falling film in a cross flow configuration, International Journal of Heat and Mass Transfer, 47 (2004) 743-755.
[27] Ali A., Vafai K., An investigation of heat and mass transfer between air and desiccant film in an inclined parallel and counter flow channels, International Journal of Heat and Mass Transfer, 47 (2004) 1745-1760.
[28] Solangi K., Kazi S., Luhur M., Badarudin A., Amiri A., Sadri R., Zubir M., Gharehkhani S., Teng K., A comprehensive review of thermo-physical properties and convective heat transfer to nanofluids, Energy, 89 (2015) 1065-1086.
[29] Wen T., Lu L., Dong C., Luo Y., Development and experimental study of a novel plate dehumidifier made of anodized aluminum, Energy, 144 (2018) 169-177.
[30] Conde M.R., Properties of aqueous solutions of lithium and calcium chlorides: formulations for use in air conditioning equipment design, International Journal of Thermal Sciences, 43 (2004) 367-382.
[31] Coleman H.W., Steele W.G., Experimentation, validation, and uncertainty analysis for engineers, John Wiley & Sons, 2009.
[32] Wen T., Lu L., Dong C., Luo Y., Investigation on the regeneration performance of liquid desiccant by adding surfactant PVP-K30, International Journal of Heat and Mass Transfer, 123 (2018) 445-454.
[33] Dong C., Lu L., Wen T., Experimental study on dehumidification performance enhancement by TiO2 superhydrophilic coating for liquid desiccant plate dehumidifiers, Building and Environment, 124 (2017) 219-231.
[34] Liu J., Zhang T., Liu X., Jiang J., Experimental analysis of an internally-cooled/heated liquid desiccant dehumidifier/regenerator made of thermally conductive plastic, Energy and Buildings, 99 (2015) 75-86.
[35] Lemmon E., Huber M., McLinden M., REFPROP: Reference fluid thermodynamic and transport properties, NIST standard reference database, 23 (2007).